



Spline-based deconvolution

Amir Averbuch*, Valery Zheludev

School of Computer Science, Tel Aviv University, Tel Aviv 69978, Israel

ARTICLE INFO

Article history:

Received 27 July 2008

Received in revised form

15 March 2009

Accepted 18 March 2009

Available online 5 April 2009

Keywords:

Spline deconvolution

2D data

Noised data

Harmonic analysis

Approximate solutions

ABSTRACT

This paper proposes robust algorithms to perform deconvolution and inversion of the heat equation starting from 1D and 2D discrete noised data. The solutions are provided as splines that minimize some parameterized quadratic functionals. Parameters choice determines the trade-off between the regularity of the solution and the approximation of the initial data. The solutions are derived in an explicit form that uses aversion of harmonic analysis in splines spaces. The presented algorithms are easily implemented in a fast way while providing stable approximate solutions that restore the exact solutions with high accuracy even when the initial data are severely corrupted by noise. The approximate solutions have the same smoothness as the exact solution. The convergence of the approximate solutions to the exact solutions is proved when the sampling rate and the signals-to-noise ratios increase.

© 2009 Elsevier B.V. All rights reserved.

1. Introduction

Deconvolution is a required operation in many signal processing applications such as system identification, spectroscopy, seismic processing, image deblurring, to name a few. This is an active area of research with many publications. No universal algorithm has been developed so far. The reason lies in a diversity of applications and in the intrinsic ill-posedness of the problem. The ill-posedness of the problem stems from the fact that direct convolution of a signal (in applications convolution means measuring a signal by an instrument, transmission through a channel, propagation of a seismic signal through the earth, observation of a distant or small object through optical device) results in smoothing. Measurements of the convolved signal are typically available in a discrete set of points and comprise errors. Thus, a straightforward inversion of the convolution operator leads to an amplification of these errors. Therefore, this inversion is far from being stable and robust. A number of approaches have been suggested to overcome this

instability starting from the classical work by Wiener [16]. Recently, wavelet based methods were presented [4,3,6]. However, by now, most efficient deconvolution algorithms are based on the Tikhonov regularization method [14,15] and related schemes [11,8]. Wavelets and regularization methods were combined in [10].

Tikhonov methodology, in which approximate solution is derived as a minimizer of a certain parameterized functional, provides a trade-off between the approximation of the given data and the regularity of the solution. Naturally, in problems where the convolution is involved, the Fourier transform is widely used. However, in signal processing applications, some contradiction exists between continuous convolution, which physical devices produce, and the discreteness of the available data. Spline functions enable to overcome this contradiction by mapping the discrete data into spaces of smooth functions. An additional advantage of using splines for deconvolution application lies in their abilities to effectively control the smoothness of the solution.

In this paper, we present spline-based algorithms for solving the convolution integral equation and inverting the heat equation. Both problems are closely related. For the latter problem, we suggest solution schemes, which imply either the collocation or a finite difference

* Corresponding author.

E-mail address: amir@math.tau.ac.il (A. Averbuch).

approximation. The algorithms are based on Tikhonov regularization. Our working tool is a version of harmonic analysis in spaces of periodic splines. This analysis was developed in [18,21]. Orthogonal bases of spline spaces are designed. Their properties are similar to the properties of Fourier harmonics. These bases perfectly match the solution of convolution-related problems. The usage of these bases provides an efficient computation scheme to derive explicit solutions and the tools to flexibly control their properties. In addition, this harmonic analysis appears useful for the construction of wavelet transforms in spline spaces [21,2]. A non-periodic version of this harmonic analysis was presented in [22,23].

The paper is organized as follows. In Section 2, we formulate the problems to be solved and provide some necessary facts about periodic splines. In Section 3, we outline the spline harmonic analysis. Stable approximate solutions to the standard convolution equation in one and two dimensions are derived in Section 4. The same is done for the inversion of the heat equation in Section 5. Section 6 presents numerical results from the experiments in solving convolution and inverse heat equations starting from the strongly noised discrete data. Appendix A describes how to calculate spline values at the inner points between its nodes. The convergence of the approximate solutions to the exact solutions is proved in Appendix B.

2. Preliminaries

2.1. Notation and formulation of the problems

The convolution equation is

$$g(x) = \int_{-\infty}^{\infty} h(x-s)f(s) ds. \tag{2.1}$$

Here f is an unknown sought after function, h is the kernel and g is the given data function. If the functions h and g are compactly supported then, necessarily, the unknown function f has a compact support as well. In this case, the problem can be reduced to finding a 1-periodic solution of the following equation:

$$g(x) = h \star f(x) \triangleq \int_0^1 h(x-y)f(y) dy, \tag{2.2}$$

where the functions h and g are 1-periodic and \star denotes the convolution operator.

Problem C. Given two 1-periodic functions g and h , find 1-periodic functions f that satisfy Eq. (2.2).

Inverting the heat equation, which is an ill-conditioned problem, is closely related to solving the convolution Eq. (2.2).

Let a 1-periodic function $f(x)$ belong to the space C^m , which is the space of 1-periodic functions that have continuous derivatives up to order m . Denote by \mathbf{U}_t the linear operator such that $\mathbf{U}_t f(x) = u(x, t)$ where $u(x, t)$ is the solution of the heat equation

$$\frac{\partial u(x, t)}{\partial t} = u_x''(x, t), \quad u(x, 0) = f(x). \tag{2.3}$$

Problem I. Let t be a fixed time parameter. Given $g(x) = \mathbf{U}_t f(x)$, find $f(x)$.

In most practical applications, the data function $g(x)$ is sampled on a grid $\{x_k\}$. Typically, the samples are corrupted by a random noise $\{e_k\}$. Then, only approximate solutions are possible.

In this paper, we assume that the grid is uniform $\{x_k = k/N\}$, where $N = 2^j$, $j \in \mathbb{N}$. In addition, we assume that only samples of a periodic kernel h on the grid $\{k/N\}$ are known. Thus, when Problem C is handled, we have at our disposal N -periodic sequences \mathbf{z} and \mathbf{h} such that $\mathbf{z} = \mathbf{g} + \mathbf{e}$, $\mathbf{g} \triangleq \{g(k/N)\}$, $\mathbf{e} \triangleq \{e_k\}$ and $\mathbf{h} \triangleq \{h(k/N)\}$. In the case of Problem I, the data are $\mathbf{z} = \mathbf{g} + \mathbf{e}$, $\mathbf{g} \triangleq \{g(k/N) = \mathbf{U}_t f(x)_{x=k/N}\}$ and $\mathbf{e} \triangleq \{e_k\}$. We assume that the kernel is $h \in C^l$ and the data function is $g \in C^{l+m}$. The error sequences \mathbf{e} are assumed to have zero mean such that $\text{var}(\mathbf{e}) \leq \varepsilon^2$.

The norm of an N -periodic sequence $\mathbf{a} \triangleq \{a_k\}$ is defined by $\|\mathbf{a}\| \triangleq \sqrt{\sum_k a_k^2}$. From now on, \sum_k stands for $\sum_{k=0}^{N-1}$. The norm of a 1-periodic function f is $\|f\| \triangleq \sqrt{\int_0^1 f^2(x) dx}$.

Denote $\omega \triangleq e^{2\pi i/N}$. The direct and the inverse discrete Fourier transforms (DFT's) of an N -periodic signal $\mathbf{a} \triangleq \{a_k\}$ are

$$\hat{a}(n) \triangleq \sum_k \omega^{-kn} a_k, \quad a_k = \frac{1}{N} \sum_n \omega^{kn} \hat{a}(n).$$

The circular discrete convolution $\mathbf{c} \triangleq \{c_k\}$ of periodic signals \mathbf{a} and $\mathbf{b} \triangleq \{b_k\}$ and its DFT are connected by

$$\mathbf{c} = \mathbf{a} \star \mathbf{b} \iff c_k = \sum_l a_{k-l} b_l \iff \hat{c}(n) = \hat{a}(n) \hat{b}(n).$$

We propose to find approximate solutions to Problems C and I in the form of periodic splines of order p . The discrete Fourier transform and a version of harmonic analysis in the spline space will be utilized for the construction of such splines.

2.2. Periodic splines

The function

$$\tilde{B}_N^1(x) \triangleq \begin{cases} N, & x \in [-1/2N, 1/2N], \\ 0 & \text{otherwise,} \end{cases}$$

is called the centered B-spline of first order on the grid $\{k/N\}$. The periodization of the spline $B^1(x) \triangleq \sum_{l \in \mathbb{Z}} \tilde{B}_N^1(x+l)$ is called the periodic B-spline of first order on the grid $\{k/N\}$. Its Fourier coefficients are

$$C_n(B^1) \triangleq \int_0^1 e^{-2\pi i n x} B^1(x) dx = \frac{\sin(\pi n/N)}{\pi n/N}.$$

The periodic B-spline of order p is defined via the iterated circular convolution $B^p(x) \triangleq B^1(x) \star B^{p-1}(x)$. Its Fourier coefficients are

$$C_n(B^p) = (C_n(B^1))^p \iff B^p(x) = \sum_{n=-\infty}^{\infty} \left(\frac{\sin(\pi n/N)}{\pi n/N} \right)^p e^{2\pi i n x}. \tag{2.4}$$

The B-spline $B^p(x)$ is symmetric about zero and non-negative. Its support (up to periodization) is $(-p/2N, p/2N)$.

The spline $B^p(x)$ consists of pieces of polynomials of degree $p - 1$ that are linked to each other at the nodes $\{(2k + p)/2N\}$ such that $B^p(x)$ belongs to the space C^{p-2} . The definition of $B^p(x)$ implies that

$$B^p \star B^m(x) = B^{p+m}(x) \in C^{p+m-2}. \tag{2.5}$$

Translations of the B-spline $B^p(x)$ form a basis in the space \mathcal{S}^p of periodic splines of order p defined on the grid $\{k/N\}$. A spline $S^p(x) \in \mathcal{S}^p$ and its Fourier coefficients are

$$S^p(x) = \sum_{k \in \mathbb{Z}} q_k B^p\left(x - \frac{k}{N}\right),$$

$$C_n(S^p) = \hat{q}(n)C_n(B^p) = \hat{q}(n)\left(\frac{\sin(\pi n/N)}{\pi n/N}\right)^p, \tag{2.6}$$

where $\mathbf{q} \triangleq \{q_k\}$ is a N -periodic sequence. It follows from (2.5) that the convolution of two periodic splines

$$S_1^p \star S_2^m(x) = S_3^{p+m}(x) \in C^{p+m-2}, \tag{2.7}$$

is a spline, whose order is equal to the sum of the orders of the convolved splines.

3. Harmonic analysis of periodic splines

3.1. Exponential splines

In this section, an orthogonal basis in the space \mathcal{S}^p of periodic splines is constructed. This basis resembles the Fourier basis of the space of periodic functions consisting of complex exponential functions. Originally, this construction was presented in its final form in [21] but some of its components were exposed in [18,19].

Let a spline $S^p \in \mathcal{S}^p$ be represented as in (2.6). We can write $q_k = N^{-1} \sum_n \omega^{nk} \hat{q}(n)$. Substituting it to (2.6), we get

$$S^p(x) = \frac{1}{N} \sum_k B^p(x - k/N) \sum_n \omega^{nk} \hat{q}(n) = \frac{1}{N} \sum_n \hat{q}(n) \beta_n^p(x), \tag{3.1}$$

where

$$\beta_n^p(x) \triangleq \sum_k \omega^{-nk} B^p(x + k/N) \iff B^p(x + k/N)$$

$$= \frac{1}{N} \sum_n \omega^{nk} \beta_n^p(x). \tag{3.2}$$

The functions $\beta_n^p(x)$ are splines from the space \mathcal{S}^p , whose coefficients in the B-spline basis are $\{\omega^{nk}\}$. The spline sequence $\{\beta_n^p(x)\}$ is N -periodic with respect to n . Thus, the spline $\beta_n^p(x)$ can be interpreted as a periodic version of the Zak transform [7,17] of the B-spline $B^p(x)$. We call them the *exponential splines*. The non-periodic exponential splines were introduced by Schoenberg [12, p. 17]. Eq. (2.6) implies that the Fourier coefficients of exponential splines

$$C_m(\beta_n^p) = \left(\frac{\sin \pi m/N}{\pi m/N}\right)^p \sum_k \omega^{-k(m-n)}$$

$$= N \delta_n^m(\text{mod } N) \left(\frac{\sin \pi m/N}{\pi m/N}\right)^p, \tag{3.3}$$

where δ_n^m is the Kronecker delta. Hence, it follows that:

$$\beta_n^p(x) = N \sum_{m=-\infty}^{\infty} e^{2\pi i(n+mN)x} \left(\frac{\sin(\pi(n+mN)/N)}{\pi(n+mN)/N}\right)^p. \tag{3.4}$$

For further use, we single out the N -periodic sequences

$$u_n^p \triangleq \frac{\beta_n^p(0)}{N} = \frac{1}{N} \sum_k \omega^{-nk} B^p\left(\frac{k}{N}\right)$$

$$= \sin^p \frac{\pi n}{N} \sum_{m=-\infty}^{\infty} \frac{(-1)^{pm}}{(\pi(n+mN)/N)^p}. \tag{3.5}$$

These sequences can be explicitly calculated via the application of the DFT to the values of B-splines. They are closely related to Euler–Frobenius polynomials [12]. It is important for us that the sequences u_n^p are strictly positive and

$$0 < U_p \leq u_{N/2}^p \leq u_n^p \leq u_0^p = 1. \tag{3.6}$$

The constants U_p do not depend on N and $\lim_{p \rightarrow \infty} U_p = 0$.

Examples.

$$u_n^2 \equiv 1, \quad u_n^3 = \frac{1 + \cos^2 \frac{\pi n}{N}}{2}, \quad u_n^4 = \frac{1 + 2\cos^2 \frac{\pi n}{N}}{3},$$

$$u_n^6 = \frac{2 + 11\cos^2 \frac{\pi n}{N} + 2\cos^4 \frac{\pi n}{N}}{15}.$$

3.1.1. Properties of the splines β_n^p

Basis: The splines $\{\beta_n^p\}_{n=0}^{N-1}$ form a basis for the space \mathcal{S}^p . It follows immediately from (3.1) and (3.2).

Orthogonality: Let β_n^p and β_r^q be exponential splines of orders p and q . Due to Parseval identity and Eq. (3.3), the inner product becomes

$$\langle \beta_n^p, \beta_r^q \rangle \triangleq \int_0^1 \beta_n^p(x) \overline{\beta_r^q(x)} dx = \sum_{m=-\infty}^{\infty} C_m(\beta_n^p) \overline{C_m(\beta_r^q)}$$

$$= N^2 \sum_{m=-\infty}^{\infty} \delta_n^m(\text{mod } N) \delta_r^m(\text{mod } N) \left(\frac{\sin \pi m/N}{\pi m/N}\right)^{p+q}$$

$$= N^2 \delta_n^r u_n^{p+q}. \tag{3.7}$$

Eq. (3.7) implies, in particular, that the exponential splines $\{\beta_n^p\}_{n=0}^{N-1}$ form an orthogonal basis for the space \mathcal{S}^p and their norms are $\|\beta_n^p\| = \sqrt{\int_0^1 |\beta_n^p(x)|^2 dx} = N \sqrt{u_n^{2p}}$.

Shift: It follows from (3.2) that the shifts of the exponential splines are

$$\beta_n^p(x + l/N) = \sum_k \omega^{-nk} B^p(x + (k+l)/N) = \omega^{ln} \beta_n^p(x). \tag{3.8}$$

Eq. (3.8) means that, like the discrete exponential functions $\{e^{2\pi i n t/N}\}$, the exponential splines are the eigenfunctions of the operator of shifts on the grid $\{k/N\}$.

Differentiation: The continuous exponential functions $\{e^{2\pi i n x}\}$ are the eigenfunctions of the differentiation operator. The exponential splines possess a similar property. Eq. (3.4) implies that

$$\beta_n^p\left(x - \frac{p}{2N}\right)^{(s)} = N^s (1 - \omega^{-n})^s \beta_n^{p-s}\left(x - \frac{p-s}{2N}\right). \tag{3.9}$$

The spline β_n^{p-s} is a replica of the exponential spline $\beta_n^p \in \mathcal{S}^p$ in the space \mathcal{S}^{p-s} .

Convolution: If two periodic functions h and f are convolved $g = h \star f$, then their Fourier coefficients are: $C_n(g) = C_n(h)C_n(f)$. This fact, together with Eq. (3.3), imply that

$$\beta_n^p \star \beta_r^s = N \delta_r^p \beta_n^{p+s}. \quad (3.10)$$

This property is similar to the corresponding property of exponential functions.

Interpolation: To further highlight the relationship between exponential splines and exponential functions, we argue that the exponential splines interpolate the exponential functions at grid points. To be specific, Eq. (3.8) implies that

$$\beta_n^p(l/N) = \omega^{ln} \beta_n^p(0) \implies \frac{\beta_n^p(l/N)}{N u_n^p} = \exp(2\pi i n l / N).$$

3.2. Representation of periodic splines in exponential basis

Section 3.1 established that any spline $S^p \in \mathcal{S}^p$ can be expanded via the orthogonal basis $\{\beta_n^p\}_{n=0}^{N-1}$ as

$$S^p(x) = \frac{1}{N} \sum_n \xi_n \beta_n^p(x), \quad \xi_n \triangleq \hat{q}(n). \quad (3.11)$$

This expansion imposes a harmonic analysis methodology on the spline space, where the exponential splines $\{\beta_n^p(x)\}_{n=0}^{N-1}$ play the harmonics part. We list basic formulas from this analysis, which are similar to classical harmonic analysis formulas.

Parseval identity: Let the $S^p \in \mathcal{S}^p$ be represented as in (3.11) and

$$S^r(x) = \frac{1}{N} \sum_m \eta_m \beta_m^r(x) \in \mathcal{S}^r. \quad (3.12)$$

Then, due to (3.7),

$$\begin{aligned} \langle S^p, S^r \rangle &= \frac{1}{N^2} \sum_{n,m} \xi_n \bar{\eta}_m \langle \beta_n^p, \bar{\beta}_m^r \rangle = \sum_n \xi_n \bar{\eta}_n u_n^{p+r}, \\ \|S^p\|^2 &= \sum_n |\xi_n|^2 u_n^{2p}. \end{aligned} \quad (3.13)$$

Convolution: Let the $S^p \in \mathcal{S}^p$ and $S^r \in \mathcal{S}^r$ be represented as in (3.11) and (3.12), respectively.

Then, due to (3.10),

$$\begin{aligned} S^p \star S^r(x) &= \frac{1}{N^2} \sum_{n,m} \xi_n \eta_m \beta_n^p \star \beta_m^r(x) \\ &= \frac{1}{N} \sum_n \xi_n \eta_n \beta_n^{p+r}(x) \in \mathcal{S}^{p+r}. \end{aligned} \quad (3.14)$$

Thus, the ‘‘Fourier coefficients’’ are multiplied as in the classical harmonic analysis.

Differentiation: Let the $S^p \in \mathcal{S}^p$ be represented as in (3.11). Then, by combining Eq. (3.9) with the Parseval identity (3.13), we obtain

$$\begin{aligned} \|(S^p)^{(s)}\|^2 &= N^{2s} \sum_n |1 - \omega^{-n}|^{2s} |\xi_n|^2 u_n^{2(p-s)} \\ &= \sum_n w_n^{2s} |\xi_n|^2 u_n^{2(p-s)}, \quad w_n \triangleq 2N \sin\left(\frac{\pi n}{N}\right). \end{aligned} \quad (3.15)$$

Interpolation: Let the spline $S^p \in \mathcal{S}^p$, which is represented as in (3.11), interpolate the data $\{z_k\}$ on the grid $\{k/N\}$. Then, due to (3.8),

$$\begin{aligned} S^p(k/N) &= \frac{1}{N} \sum_n \xi_n \beta_n^p(k/N) = z_k \iff \sum_n \xi_n \omega^{kn} u_n^p \\ &= z_k \iff \xi_n = \frac{\hat{z}(n)}{N u_n^p}. \end{aligned} \quad (3.16)$$

Thus, the discrete Parseval identity follows:

$$\frac{1}{N} \sum_k |S^p(k/N)|^2 = \sum_n |\xi_n|^2 (u_n^p)^2. \quad (3.17)$$

Comparing the continuous Parseval identity (3.13) with the discrete one (3.17), we get the inequality

$$\begin{aligned} \|S^p\|^2 &= \sum_n |\xi_n|^2 u_n^{2p} = \sum_n |\xi_n|^2 (u_n^p)^2 \frac{u_n^{2p}}{(u_n^p)^2} \\ &\leq \frac{1}{U_p^2} \sum_n |\xi_n|^2 (u_n^p)^2 = U_p^{-2} \frac{1}{N} \sum_k |S^p(k/N)|^2. \end{aligned} \quad (3.18)$$

The constant U_p is defined in Eq. (3.6).

4. Solving the convolution equation

In this section, we provide an approximate solution to Problem C. For that, we solve an auxiliary problem.

4.1. Solving an auxiliary problem

Assume $\mathbf{z} = \{z_k\}$ and $\mathbf{h} = \{h(k/N)\}_{k=0}^{N-1}$ are data arrays, $S^r \in \mathcal{S}^r$ is the spline, which interpolates the sampled kernel \mathbf{h} and ρ is a numerical parameter.

Problem MFC. Find a spline $S^p \in \mathcal{S}^p$, which minimizes the functional $J_\rho(S^p) \triangleq \rho I(S^p) + E(S^p)$, where

$$\begin{aligned} I(S^p) &\triangleq \sum_{s=0}^m \|(S^p)^{(s)}\|^2, \\ E(S^p) &\triangleq \frac{1}{N} \sum_k (S^r \star S^p(k/N) - z_k)^2. \end{aligned} \quad (4.1)$$

Assume that $S^p \in \mathcal{S}^p$ and $S^r \in \mathcal{S}^r$ are represented as in (3.11) and (3.12), respectively. Eq. (3.13) implies that

$$I(S^p) = \sum_n |\xi_n|^2 D_n^m, \quad D_n^m \triangleq \sum_{s=0}^m w_n^{2s} u_n^{2(p-s)}. \quad (4.2)$$

We derive from Eqs. (3.14) and (3.16) that

$$\begin{aligned} S^p \star S^r(k/N) - z_k &= \frac{1}{N} \sum_n \xi_n \eta_n \beta_n^{p+r}(k/N) - z_k \\ &= \frac{1}{N} \sum_n \omega^{kn} (\xi_n \eta_n N u_n^{p+r} - \hat{z}(n)) \\ \implies E(S^p) &= \frac{1}{N^2} \sum_n |\xi_n \eta_n N u_n^{p+r} - \hat{z}(n)|^2. \end{aligned} \quad (4.3)$$

Consequently, the functional $J_\rho(S^p)$ can be presented as follows

$$J_\rho(S^p) = \sum_n (\rho |\xi_n|^2 D_n^m + |\xi_n \eta_n u_n^{p+r} - \hat{z}(n)/N|^2).$$

Thus, the solution to Problem MFC is the spline $S_\rho^p \in \mathcal{S}^p$

$$S_\rho^p = \frac{1}{N} \sum_n \xi_n(\rho) \beta_n^p(x) = \sum_{k \in \mathbb{Z}} q_k(\rho) B^p\left(x - \frac{k}{N}\right),$$

$$q_k(\rho) = \frac{1}{N} \sum_n \omega^{kn} \xi_n(\rho), \tag{4.4}$$

$$\xi_n(\rho) = \frac{\bar{\eta}_n \hat{z}(n) u_n^{p+r}}{N A_n(\rho)},$$

$$A_n(\rho) \triangleq \rho \sum_{s=0}^m w_n^{2s} u_n^{2(p-s)} + (|\eta_n| u_n^{p+r})^2. \tag{4.5}$$

4.2. Approximate solutions to the convolution equation

The spline $S_\rho^p(x)$, $p = 2m$, which is defined by Eqs. (4.4) and (4.5), provides an approximate solution to Problem C in the following sense:

Theorem 4.1. Assume that the function f belongs to C^m , the function h belongs to C^l and $g(x) = h \star f(x)$. Then, $g \in C^{l+m}$. If the discretization step $1/N \rightarrow 0$ and the variance of the error vector $\text{var}(\mathbf{e}) \rightarrow 0$ then there exists a scheme for selection of the parameter $\rho(N, e)$ such that

$$\max_{j=0:m-1} \max_{x \in [0,1]} |S_{\rho(N,e)}^{2m}(x)^{(j)} - f^{(j)}(x)| \rightarrow 0 \text{ as } N \rightarrow \infty, e \rightarrow 0.$$

This theorem will be proved in Appendix B.

Assume we have \mathbf{z} and \mathbf{h} as the data. Then, a practical scheme for the selection of the parameter ρ , which is based on a priori estimate of the variance of errors vector \mathbf{e} and on the regularity of the solution $f(x)$, is the following.

Let $E(S^p)$ and $I(S^p)$ be the functionals defined in Eq. (4.1) and let ε be a numerical parameter.

Problem MIC. Find a spline $S_\rho^p \in \mathcal{S}^p$ that minimizes the functional $I(S^p)$ under the constraint $E(S^p) \leq \varepsilon^2$.

Denote $e(\rho) \triangleq E(S_\rho^p)$ where S_ρ^p is the spline presented in Eqs. (4.4) and (4.5). It can happen that some $\eta_n = 0$. Then, denote by θ the set of indices where $\eta_n = 0$. If θ is not empty then denote $\mu(z) \triangleq \sum_{n \in \theta} |z(n)|^2$. It follows from Eqs. (4.3)–(4.5) that

$$e(\rho) = \sum_n \left(\frac{\rho D_n^m |\hat{z}(n)|}{N A_n(\rho)} \right)^2 = \frac{1}{N^2} \left(\sum_{n \notin \theta} \left(\frac{\rho D_n^m |\hat{z}(n)|}{A_n(\rho)} \right)^2 + \mu(z) \right).$$

Its derivative

$$e'(\rho) = \frac{1}{N^2} \sum_{n \notin \theta} \frac{2\rho |D_n^m \eta_n \hat{z}(n) u_n^{p+r}|^2}{(A_n(\rho))^3} > 0,$$

is strictly positive. Consequently, the function $e(\rho)$ grows strictly monotonically, while $e(0) = N^{-2} \mu(z)$ and $\lim_{\rho \rightarrow \infty} e(\rho) = N^{-1} \|\mathbf{z}\|^2$.

Hence, it follows that for any $\varepsilon < N^{-1/2} \|\mathbf{z}\|$, Problem MIC has a unique solution $S_\rho^p \in \mathcal{S}^p$. This solution $S_\rho^p(x) = S_\rho^p(x)$, where the spline S_ρ^p was presented in Eqs. (4.4) and (4.5) and the value of the parameter ρ is determined by the

following equation:

$$e(\rho) = \sum_{n \notin \theta} \left(\frac{\rho D_n^m |\hat{z}(n)|}{A_n(\rho)} \right)^2 + \mu(z) = \varepsilon^2. \tag{4.6}$$

Assume that the variance’s estimate of the zero-mean error vector $N^{-1} \sum_k e_k^2 = \varepsilon^2$ is known. Then, it is reasonable to require $E(S^p) \leq \varepsilon^2$ while searching for the “most regular” (in the sense of minimal $I(S^p)$) spline that satisfies this condition. The spline S_ρ^p provides this suboptimal approximate solution.

For further use, we introduce the function

$$i(\rho) \triangleq I(S_\rho^p) = \sum_{n \notin \theta} \frac{D_n^m |\eta_n \hat{z}(n)|^2}{(\rho D_n^m + (|\eta_n| u_n^{p+r})^2)}. \tag{4.7}$$

This function decays strictly monotonically, while $\lim_{\rho \rightarrow \infty} i(\rho) = 0$ and

$$i(0) = C \triangleq \sum_{n \notin \theta} D_n^m \left(\frac{|\hat{z}(n)|}{|\eta_n| u_n^{p+r}} \right)^2.$$

Remarks on evaluation of the noise variance. Assume that the index set θ is not empty and comprises M terms: $\theta = \{\theta_m\}_{m=1}^M$. Then, the entries of the sum $\mu(z) \triangleq \sum_{n \in \theta} |z(n)|^2$ are related to the zero-mean noise component $\mathbf{e} = \{e_k\}$ of the data $\{z_k = g(k/N) + e_k\}$. Thus, the estimation

$$\begin{aligned} \text{var}(\mathbf{e}) &= \frac{1}{N} \sum_k e_k^2 = \frac{1}{N^2} \sum_n |\hat{e}(n)|^2 \\ &= \frac{1}{N^2} \left(\sum_{n \notin \theta} |\hat{e}(n)|^2 + \sum_{m=1}^M |\hat{e}(\theta_m)|^2 \right) \\ &= \frac{1}{N^2} \left(\sum_{n \notin \theta} |\hat{e}(n)|^2 + \mu(z) \right). \end{aligned}$$

If the error sequence is the white noise then its energy is spread near uniformly over all N frequencies. Thus, if the quantity M is not too small compared to N then we can evaluate the variance

$$\varepsilon^2 \approx \frac{1}{N^2} \mu(z) \frac{N}{M} = \frac{\mu(z)}{MN}. \tag{4.8}$$

A typical case is when, formally, the set θ is empty but many of the coordinates η_n of the kernel are negligible small. In this case, the reasoning leading to the estimation (4.8) remains true while we replace the set θ by the set $\tilde{\theta}$ of indices where $\eta_n \approx 0$.

4.3. Outline of the 2D case

The 2D convolution equation with the functions, which are 1-periodic in both vertical and horizontal directions, is

$$g(x, y) = h \star f(x, y) \triangleq \int_0^1 \int_0^1 h(x - s, y - t) f(s, t) ds dt. \tag{4.9}$$

Here, \star denotes the 2D convolution operator. In this section, the term periodic means 1-periodicity in both directions.

Problem C2. Given two periodic functions g and h , find the periodic functions f that satisfy Eq. (4.9).

We assume that the data are sampled on the grid $\{\gamma_{k,n} = (k/N, n/N)\}$. The samples are corrupted by a random noise $\{e_{k,n}\}$. In addition, we assume that only samples from the periodic kernel h on the grid $\{\gamma_{k,n}\}$ are known. Thus, we have at our disposal N -periodic arrays \mathbf{z} and \mathbf{h} such that $\mathbf{z} = \mathbf{g} + \mathbf{e}$, $\mathbf{g} \triangleq \{g(k/N, n/N)\}$, $\mathbf{e} \triangleq \{e_{k,n}\}$ and $\mathbf{h} \triangleq \{h(k/N, n/N)\}$.

We assume that the kernel $h \in C^l$, which means that it has continuous derivatives up to order l in both directions, and the data function $g \in C^{l+m}$. The error sequences \mathbf{e} are assumed to have zero mean such that $\text{var}(\mathbf{e}) < \varepsilon^2$. The norm of an N -periodic array $\mathbf{a} \triangleq \{a_{k,n}\}$ is defined by $\|\mathbf{a}\| \triangleq \sqrt{\sum_{k,n} a_{k,n}^2}$. In this section, $\sum_{k,n}$ stands for $\sum_{k,n=0}^{N-1}$. The norm of a periodic function f is $\|f\| \triangleq \sqrt{\int_0^1 \int_0^1 f^2(x, y) dx dy}$.

The direct and inverse 2D DFT's of an N -periodic array $\mathbf{a} \triangleq \{a_{k,n}\}$ are

$$\hat{a}(\kappa, \nu) \triangleq \sum_{k,n} \omega^{-k\kappa - n\nu} a_{k,n}, \quad a_{k,n} = \frac{1}{N^2} \sum_{\kappa,\nu} \omega^{k\kappa + n\nu} \hat{a}(\kappa, \nu).$$

The circular discrete convolution $\mathbf{c} \triangleq \{c_{k,n}\}$ of periodic arrays \mathbf{a} and $\mathbf{b} \triangleq \{b_{k,n}\}$ and its DFT are linked by

$$\mathbf{c} = \mathbf{a} \star \mathbf{b} \iff c_{k,n} = \sum_{l,m} a_{k-l, n-m} b_{l,m} \iff \hat{c}(\kappa, \nu) = \hat{a}(\kappa, \nu) \hat{b}(\kappa, \nu).$$

We propose to find approximate solutions to Problem C2 in the form of 2D periodic splines of order $\{p, q\}$.

We define the space $\mathcal{S}^{p,q}$ of 2D periodic splines on the grid $\{\gamma_{k,n}\}$ as the space of linear combinations

$$\begin{aligned} S^{p,q}(x, y) &= \sum_{k,n} s_{k,n} B^p(x - k/N) B^q(y - n/N) \\ &= \frac{1}{N^2} \sum_{\kappa,\nu} \zeta_{\kappa,\nu} \beta_{\kappa,\nu}^{p,q}(x, y), \quad \zeta_{\kappa,\nu} = \hat{s}(\kappa, \nu), \end{aligned} \quad (4.10)$$

where $\mathbf{s} \triangleq \{s_{k,n}\}$ is an N -periodic array, $\{\hat{s}(\kappa, \nu)\}$ is the DFT of \mathbf{s} and $\beta_{\kappa,\nu}^{p,q}(x, y) \triangleq \beta_{\kappa}^p(x) \beta_{\nu}^q(y)$ are the 2D orthogonal splines.

Assume $\mathbf{z} = \{z_{k,n}\}$ and $\mathbf{h} = \{h(k/N, n/N)\}_{k,n=0}^{N-1}$ are available data arrays, $S^{\hat{p},\hat{q}}(x, y) \in \mathcal{S}^{\hat{p},\hat{q}}$ is the spline, which interpolates the sampled kernel \mathbf{h} and ρ is a numerical parameter.

Like in 1D case, we approximate the solution of Problem C2 by the spline $S_{\rho}^{p,q}(x, y) \in \mathcal{S}^{p,q}$, which minimizes the functional $J_{\rho}(S^{p,q}) \triangleq \rho I(S^{p,q}) + E(S^{p,q})$, where

$$\begin{aligned} I(S^{p,q}) &\triangleq \sum_{s=0}^m \|(S^{p,q})_{x,y}^{(s,s)}\|^2, \\ E(S^{p,q}) &\triangleq \frac{1}{N^2} \sum_{k,n} (S^{\hat{p},\hat{q}} \star S^{p,q}(k/N, n/N) - z_{k,n})^2. \end{aligned} \quad (4.11)$$

Assume that $S^{\hat{p},\hat{q}}(x, y)$ is represented as follows:

$$S^{\hat{p},\hat{q}}(x, y) = \frac{1}{N^2} \sum_{\tilde{\kappa}, \tilde{\nu}} \eta_{\tilde{\kappa}, \tilde{\nu}} \beta_{\tilde{\kappa}, \tilde{\nu}}^{\hat{p}, \hat{q}}(x, y) \in \mathcal{S}^{\hat{p}, \hat{q}},$$

$$\eta_{\tilde{\kappa}, \tilde{\nu}} = \frac{\hat{z}(\tilde{\kappa}, \tilde{\nu})}{N^2 u_{\tilde{\kappa}}^{\hat{p}} u_{\tilde{\nu}}^{\hat{q}}}. \quad (4.12)$$

Then, the solution to the minimization problem is the spline $S_{\rho}^{p,q}(x, y) \in \mathcal{S}^{p,q}$

$$\begin{aligned} S_{\rho}^{p,q}(x, y) &= \frac{1}{N^2} \sum_{\kappa,\nu} \zeta_{\kappa,\nu}(\rho) \beta_{\kappa,\nu}^{p,1}(x, y) \\ &= \sum_{k,n \in \mathbb{Z}} s_{k,n}(\rho) B^p(x - k/N) B^q(y - n/N), \end{aligned} \quad (4.13)$$

$$\begin{aligned} s_{k,n}(\rho) &= \frac{1}{N^2} \sum_n \omega^{k\kappa + n\nu} \zeta_{\kappa,\nu}(\rho), \quad \zeta_{\kappa,\nu}(\rho) = \frac{\bar{\eta}_{\kappa,\nu} \hat{z}(\kappa, \nu) u_{\kappa}^{p+\hat{p}} u_{\nu}^{q+\hat{q}}}{N^2 A_{\kappa,\nu}(\rho)}, \\ A_{\kappa,\nu}(\rho) &\triangleq \rho \sum_{s=0}^m w_{\kappa}^{2s} w_{\nu}^{2s} u_{\kappa}^{2(p-s)} u_{\nu}^{2(q-s)} + (|\eta_{\kappa,\nu}| u_{\kappa}^{p+\hat{p}} u_{\nu}^{q+\hat{q}})^2. \end{aligned} \quad (4.14)$$

A convergence property similar to Theorem 4.1 holds for 2D splines.

Denote by θ the set of indices where $\eta_{\kappa,\nu} = 0$. If θ is not empty then denote $\mu(z) \triangleq \sum_{(\kappa,\nu) \in \theta} |z(\kappa, \nu)|^2$. Practically, the value of the parameter ρ can be derived as the solution for the following equation:

$$\sum_{\kappa,\nu \notin \theta} \left(\frac{\rho D_{\kappa,\nu}^m |\hat{z}(\kappa, \nu)|}{A_{\kappa,\nu}(\rho)} \right)^2 + \mu(z) = \varepsilon^2, \quad (4.15)$$

where $\varepsilon^2 \triangleq N^{-2} \sum_{k,n} e_{k,n}^2$ is the variance's estimate of the zero-mean error array.

5. Inversion of the heat equation

In this section, an approximate solution to Problem I is derived. This problem is closely related to the deconvolution problem and it is solved in a similar way where periodic splines are used.

5.1. Solving auxiliary problems

Denote by \mathbf{V}_t^1 the linear operator defined on the spline space \mathcal{S}^p such that $\mathbf{V}_t^1 S^p(x) = \sigma^p(x, t)$, where $\sigma(x, t)$ is the spline from \mathcal{S}^p (with respect to x), which provides a solution to the difference approximation of the heat equation

$$\frac{\partial \sigma(x, t)}{\partial t} = \delta_x^2 \sigma(x, t), \quad \sigma(x, 0) = S^p(x). \quad (5.1)$$

Here, $\delta_x^2 q(x) \triangleq N^2 (q(x - 1/N) - 2q(x) + q(x + 1/N))$ is the second central difference.

Denote by \mathbf{V}_t^2 the linear operator on \mathcal{S}^p such that $\mathbf{V}_t^2 S^p(x) = \sigma^p(x, t)$, where $\sigma(x, t)$ is the spline from \mathcal{S}^p , which satisfies the collocation conditions for the heat equation

$$\frac{\partial \sigma(k/N, t)}{\partial t} = \sigma'_x(k/N, t), \quad k = 0, \dots, N-1, \quad \sigma(x, 0) = S^p(x). \quad (5.2)$$

Actually, application of the operators $\mathbf{V}_t^{1(2)}$ to the spline $S^p \in \mathcal{S}^p$ is similar to convolving it with another spline. Let

$$S^p(x) = \sum_{k \in \mathbb{Z}} q_k B^p\left(x - \frac{k}{N}\right) = \frac{1}{N} \sum_n \xi_n \beta_n^p(x), \quad \xi_n \triangleq \hat{q}(n).$$

We seek the splines $\sigma^p(x, t) = \mathbf{V}_t^{1(2)} S^p(x)$ that have a similar form

$$\sigma^p(x, t) = \frac{1}{N} \sum_n \xi_n(t) \beta_n^p(x).$$

when the operator \mathbf{V}_t^1 is applied, it follows from Eqs. (3.8) and (5.1) that $\xi'_n(t) = N^2(\omega^n - 2 + \omega^{-n})\xi_n(x) = -w_n^2 \xi_n(t)$, where $w_n \triangleq 2N \sin(\pi n/N)$.

On the other hand, Eqs. (3.9) and (5.2) imply that the application of the operator \mathbf{V}_t^2 results in the following relations:

$$\begin{aligned} \sum_n \xi'_n(t) \beta_n^p(k/N) &= - \sum_n w_n^2 \xi_n(t) \beta_n^{p-2}(k/N) \\ \implies \xi'_n(t) &= -w_n^2 \xi_n(t) \frac{u_n^{p-2}}{u_n^p}. \end{aligned}$$

Finally, we have

$$\xi_n(t) = \xi_n \eta_n(t), \quad \eta_n(t) \triangleq \begin{cases} e^{-w_n^2 t} & \text{when } \mathbf{V}_t^1 \text{ applied} \\ e^{-w_n^2 t u_n^{p-2}/u_n^p} & \text{when } \mathbf{V}_t^2 \text{ applied.} \end{cases} \quad (5.3)$$

Thus, the application of the operators $\mathbf{V}_t^{1(2)}$ to the spline $S^p \in \mathcal{S}^p$, like convolution, results in multiplication of its coordinates ξ_n with some factors. But, unlike convolution, these operators map the space \mathcal{S}^p into itself. Consequently, the scheme for finding approximate solutions is very similar to the scheme presented in Section 4.

Problem MFH. Let t be a fixed time parameter. Find a spline $S^p_\rho \in \mathcal{S}^p$, which minimizes the functional $J_\rho(S^p) \triangleq \rho I(S^p) + E(S^p)$, where

$$I(S^p) \triangleq \sum_{s=0}^m \|(S^p)^{(s)}\|^2, \quad E(S^p) \triangleq \frac{1}{N} \sum_k (\mathbf{V}_t S^p(k/N) - z_k)^2. \quad (5.4)$$

The functional $I(S^p)$ is presented in (4.2), while

$$E(S^p) = \frac{1}{N^2} \sum_n |\xi_n \eta_n(t) N u_n^p - \hat{z}(n)|^2. \quad (5.5)$$

Consequently, the functional $J_\rho(S^p)$ can be presented as follows:

$$J_\rho(S^p) = \sum_n (\rho |\xi_n|^2 D_n^m + |\xi_n \eta_n(t) u_n^p - \hat{z}(n)/N|^2). \quad (5.6)$$

Thus, the solution to Problem MFH is the spline $S^p_\rho \in \mathcal{S}^p$

$$\begin{aligned} S^p_\rho(x) &= \frac{1}{N} \sum_n \xi_n(\rho) \beta_n^p(x) = \sum_{k \in \mathbb{Z}} q_k(\rho) B^p\left(x - \frac{k}{N}\right), \\ q_k(\rho) &= \frac{1}{N} \sum_n \omega^{kn} \xi_n(\rho), \end{aligned} \quad (5.7)$$

$$\begin{aligned} \xi_n(\rho) &= \frac{\eta_n(t) \hat{z}(n) u_n^p}{NA_n(\rho)}, \\ A_n(\rho) &\triangleq \rho \sum_{s=0}^m w_n^{2s} u_n^{2(p-s)} + (\eta_n(t) u_n^p)^2, \end{aligned} \quad (5.8)$$

where that $\eta_n(t)$ is defined in (5.3).

5.2. Approximate solutions to the inversion of the heat equation

The splines $S^p_\rho(x)$, where each operator $\mathbf{V}_t^{1(2)}$ can be used, provide approximate solutions to Problem I in the following sense:

Assume that the periodic function $f(x)$, which defines the initial condition in (2.3), belongs to $C^m, m < p$. If the discretization step $1/N \rightarrow 0$ and the variance of the error vector $\text{var}(\mathbf{e}) \rightarrow 0$ then there exists a scheme to select the parameter $\rho(N, e)$ such that

$$\max_{j=0:m-1} \max_{x \in [0,1]} |S^p_{\rho(N,e)}(x)^{(j)} - f^{(j)}(x)| \rightarrow 0 \quad \text{as } N \rightarrow \infty, e \rightarrow 0.$$

This fact was established in [20] for the case when the operator \mathbf{V}_t^2 was used. For the operator \mathbf{V}_t^1 the proof is similar.

Similarly to the convolution equation, in a practical situation, when the data \mathbf{z} is available and ε^2 estimate the variance of the errors array, the parameter ρ can be chosen as the solution to the following equation:

$$e(\rho) \triangleq \sum_n \left(\frac{\rho D_n^m |\hat{z}(n)|}{NA_n(\rho)} \right)^2 = \varepsilon^2. \quad (5.9)$$

The extension of this scheme to a 2D case is straightforward.

6. Numerical experiments

We conducted a number experiments to invert the heat equation and to solve convolution equations in one and two dimensions using synthetic as well as real data. Some of them are presented in this section.

6.1. 1D examples for heat equation

It is well-known that the solution to the heat equation

$$\frac{\partial u(x, t)}{\partial t} = u''_x(x, t), \quad -\infty < x < \infty, \quad t \geq 0, \quad u(x, 0) = f(x), \quad (6.1)$$

is

$$\begin{aligned} u(x, t) &= \int_{-\infty}^{\infty} K_t(x-y) f(y) dy, \\ K_t(x) &\triangleq \frac{\exp\left(-\frac{x^2}{4t}\right)}{\sqrt{4\pi t}}. \end{aligned} \quad (6.2)$$

If the initial function $f(x)$ has a finite support and the time parameter t is not large then the problem can be approximately treated as periodic with sufficiently large period and zero boundary conditions. The latter can be rescaled to 1-periodic setting. We apply the algorithm, which was described in Section 5, to find approximate inversions to Eq. (6.1) in two syntactic examples.

Example 1. We define the initial function $f(x)$ by the following combination of the B-splines of different

orders, $N = 256$:

$$f(x) = \frac{1}{N} \left(B^2 \left(x - \frac{1}{2} \right) + 2B^4 \left(x - \frac{1}{2} - \frac{7}{N} \right) + \frac{3}{2} B^6 \left(x - \frac{1}{2} + \frac{5}{N} \right) \right). \quad (6.3)$$

$u(x, t)$ is calculated by using a separation of variables scheme when $t = 6$. The function $f(x) = u(x, 0)$ and $u(x, 6)$ are displayed in upper row of Fig. 1. The function $u(x, 6)$, which is corrupted by a Gaussian noise (that was our given data) is displayed in the bottom row of the figure

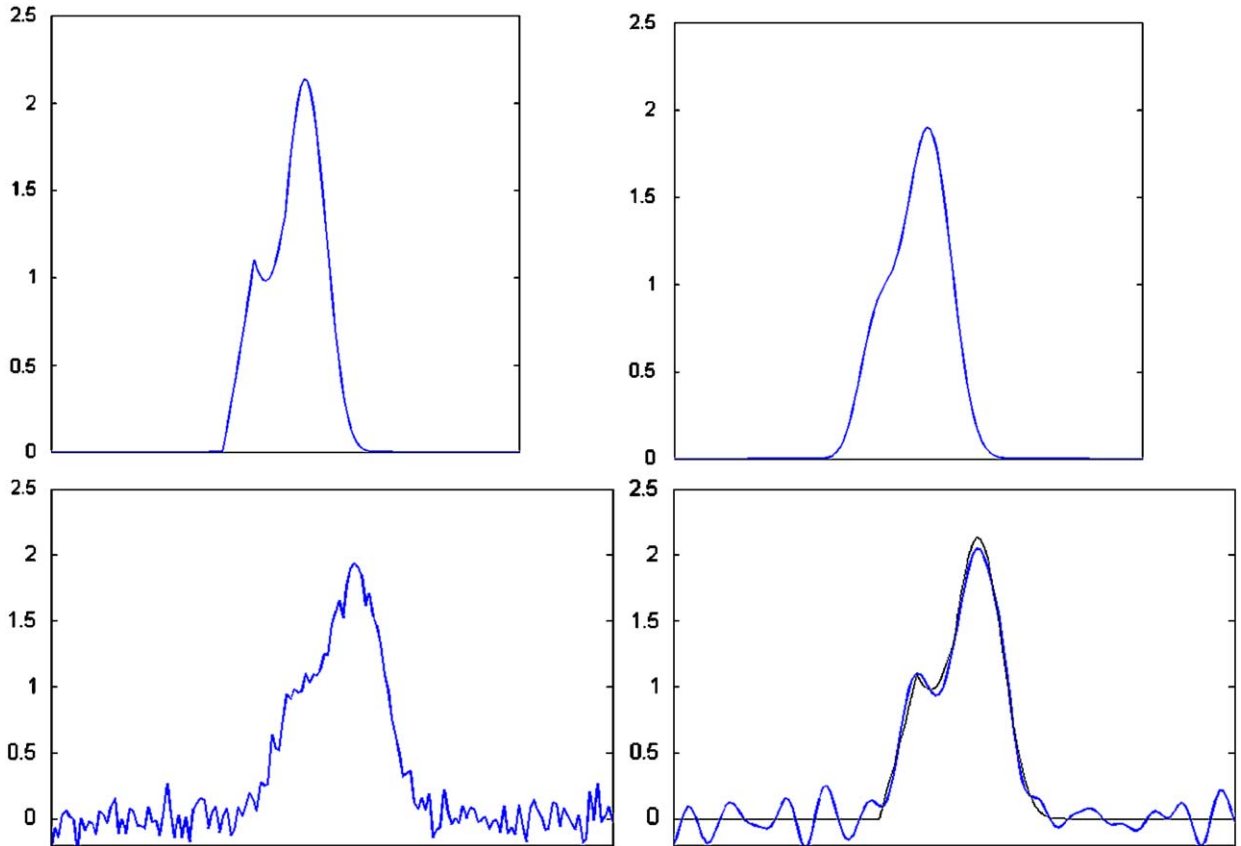


Fig. 1. Example 1. Top left: $f(x)$ (initial). Top right: $u(x, 6)$. Bottom left: the corrupted function $u(x, 6)$. Bottom right: the approximate solution $S_c^3(x)$ of the inverse problem when $t = 6$ (thick line). $f(x)$ is displayed by a thin line.

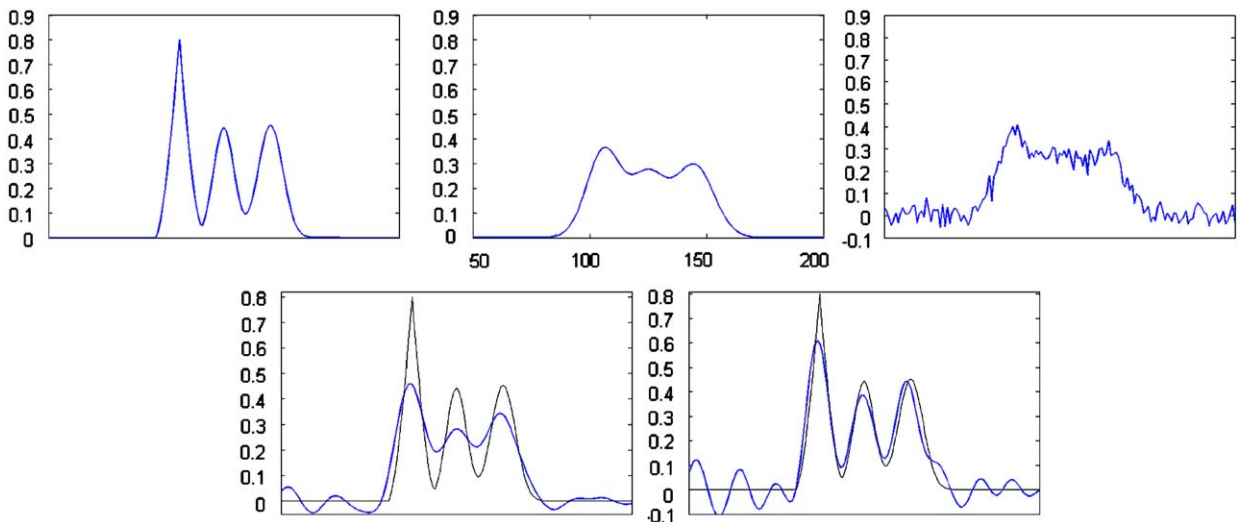


Fig. 2. Example 2. Top left: $f(x)$ (initial). Top center: $u(x, 20)$. Top right: the corrupted function $u(x, 20)$. Bottom row—approximate inversion of the heat equation from time $t = 20$. Left: the splines $S_{0.038}^2(x)$. Right: the spline $S_{0.005}^2(x)$. The function $f(x)$ is displayed by thin line.

(left). In the bottom row (right) the approximate solution of the inverse problem, which is the spline of sixth order $S_\rho^6(x)$ is displayed, where the value of the parameter $\rho = 0.02$ is determined from Eq. (5.9).

Example 2. The initial function is a combination of powers of B-splines, $N = 256$,

$$f(x) = \frac{1}{N} \left[\left(B^4 \left(x - \frac{1}{2} \right)^2 \right) + 0.8 \left(B^2 \left(x - \frac{1}{2} + \frac{16}{N} \right)^{1.5} \right) + \frac{3}{2} \left(B^6 \left(x - \frac{1}{2} - \frac{10}{N} \right)^2 \right) \right]. \quad (6.4)$$

The function $u(x, t)$ is calculated for $t = 20$. The function $f(x) = u(x, 0)$ and $u(x, 20)$ are displayed in the top row of Fig. 2. The function $u(x, 20)$, which is corrupted by Gaussian noise (that was our given data), is displayed on the right of the top row. The bottom row of Fig. 2 displays an approximate inversion of the heat equation from time $t = 20$ using the corrupted function $u(x, 20)$ (see Fig. 2) for different parameters ρ . Since the function $f(x)$ has a sharp angle, we used the linear splines $S_\rho^2(x)$. The approximate solution, where $\rho = 0.038$, which was obtained from Eq. (5.9), contains very few artifacts but it blurs the initial function $f(x)$. When ρ was reduced to $\rho = 0.005$ (right), the essential part of $f(x)$ was restored much better but some ringing artifacts emerged.



Fig. 3. Barbara. Top left: the original $f(x, y) = u(x, y, 0)$. Top right: the solution $u(x, y, 5)$, PSNR = 22.96. Center left: solution $u(x, y, 5)$ corrupted by Gaussian noise, PSNR = 22.63. Center right: inversion by the spline of fourth order PSNR = 23.53. Bottom left: solution $u(x, y, 40)$, PSNR = 20.31. Bottom right: inversion by the spline of eighth order $S_\rho^{8.8}(x, y)$, PSNR = 23.69.

6.2. 2D examples

6.2.1. 2D heat equation

We demonstrate the outputs from the inversion of the 2D heat equation by using “Barbara” as the initial function $f(x, y)$ and the available data are the pixels of the solution $u(x, y, t)$ of the heat equation

$$\frac{\partial u(x, y, t)}{\partial t} = \frac{\partial^2 u(x, y, t)}{\partial x^2} + \frac{\partial^2 u(x, y, t)}{\partial y^2}. \tag{6.5}$$

Experiment 1. Noised data. The available data are the array $\{z_{k,n} \triangleq u(k/N, n/N, 5) + e_{k,n}\}$, where $N = 512$, and

$\{e_{k,n}\}$ is Gaussian noise whose standard deviation (STD) is 5. The top row in Fig. 3 displays the initial image $f(x, y) = u(x, y, 0)$ and the solution $u(x, y, t)$ of Eq. (6.5) when $t = 5$. The middle row in Fig. 3 displays the solution $u(x, y, 5)$ corrupted by Gaussian noise whose STD = 5. The bicubic spline $S_{\rho}^{4,4}(x, y)$ restores the image by the inversion of Eq. (6.5). The parameter $\rho = 0.15$ was derived from the 2D version of Eq. (5.9). The image is restored satisfactorily.

Experiment 2. Blurred data. In this experiment, we did not add noise to the data but rather used the solution $u(x, y, t)$ at time $t = 40$ from start. Thus, the solution became highly blurred—see Fig. 3 (bottom left). The



Fig. 4. Goldhill. Top left: original $f(x, y)$. Top right: convolution with $g_{\sigma}(x, y)$, $\sigma = 3$, PSNR = 26.8. Center left: convolution with $g_3(x, y)$ corrupted by Gaussian noise, PSNR = 25.21. Center right: inversion by spline of sixth order $S_{0,0.15}^{6,6}$, PSNR = 27. Bottom left: blurred image, PSNR = 22.53. Bottom right: inversion by spline of third order $S_{\rho}^{3,3}$, PSNR = 27.74.

image in Fig. 3 (bottom right) was satisfactorily restored by the spline of eighth order $S_{\rho}^{8,8}(x,y)$ with small $\rho = 10^{-14}$ from almost indistinguishable data.

6.2.2. 2D deconvolution

Here we use the “Goldhill” image, which was represented by the function $f(x,y)$. It was convolved with different Gaussian kernels $K_{\sigma}(x,y)$.

Experiment 1: Noised convolution. The available data are the array $\{z_{k,n} \triangleq g_{\sigma}(k/N, n/N) + e_{k,n}\}$, where $g_{\sigma}(x,y) = K_{\sigma} \star$

$f(x,y)$, $N = 512$, and $\{e_{k,n}\}$ is Gaussian noise whose STD is 3. The STD σ of the kernel $K_{\sigma}(x,y)$ is 3. Fig. 4 (top row) displays the initial image $f(x,y)$ and its convolution $g_{\sigma}(x,y)$ with $\sigma = 3$.

Fig. 4 (middle row) displays the function $g_{\sigma}(x,y)$ corrupted by Gaussian noise whose STD $\sigma = 5$ and the output from the application of the spline of sixth order $S_{\rho}^{6,6}(x,y)$, which restores the image. The parameter $\rho = 0.015$ was derived from Eq. (4.15). As in the previous experiment, the presence of noise did not

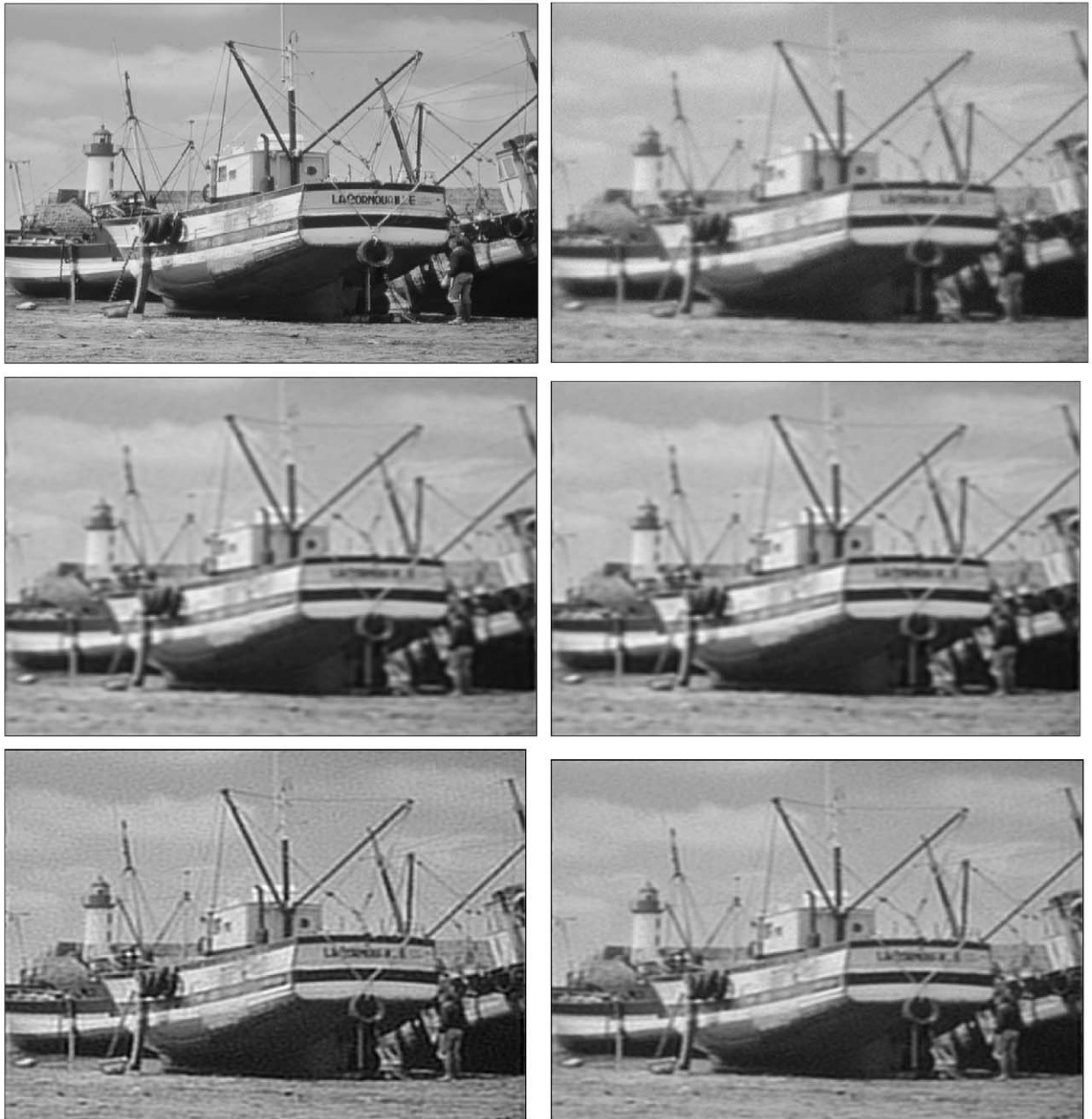


Fig. 5. “Boats” image—weak degradation. Top left: original image. Top left: blurred noised image. Center left: restored by the Wiener deconvolution. Center left: restored by the regularized deconvolution. Bottom left: restored by the spline (order 12) deconvolution. Bottom right: restored by the spline (order 2) deconvolution.

prevent to achieve a high quality restoration of the image.

Experiment 2: Blurred data. In this experiment, we did not add the noise to the data but rather used the function $g_\sigma(x, y)$, where the STD of the Gaussian kernel $K_\sigma(x, y)$ is $\sigma = 8$. Thus, the function became highly blurred.

Here, the image was satisfactorily restored from an almost indistinguishable data by the application of spline of third order $S_\rho^{3,3}(x, y)$ with a small $\rho = 10^{-15}$.

7. Discussion

We presented in Sections 4 and 5 spline algorithms for a stable approximate solution of the convolution integral equation and for the inversion of the heat equation starting from discrete noised data. The solutions are provided by the applications of splines that minimize some parameterized quadratic functionals. A choice of the parameter determines the trade-off between the

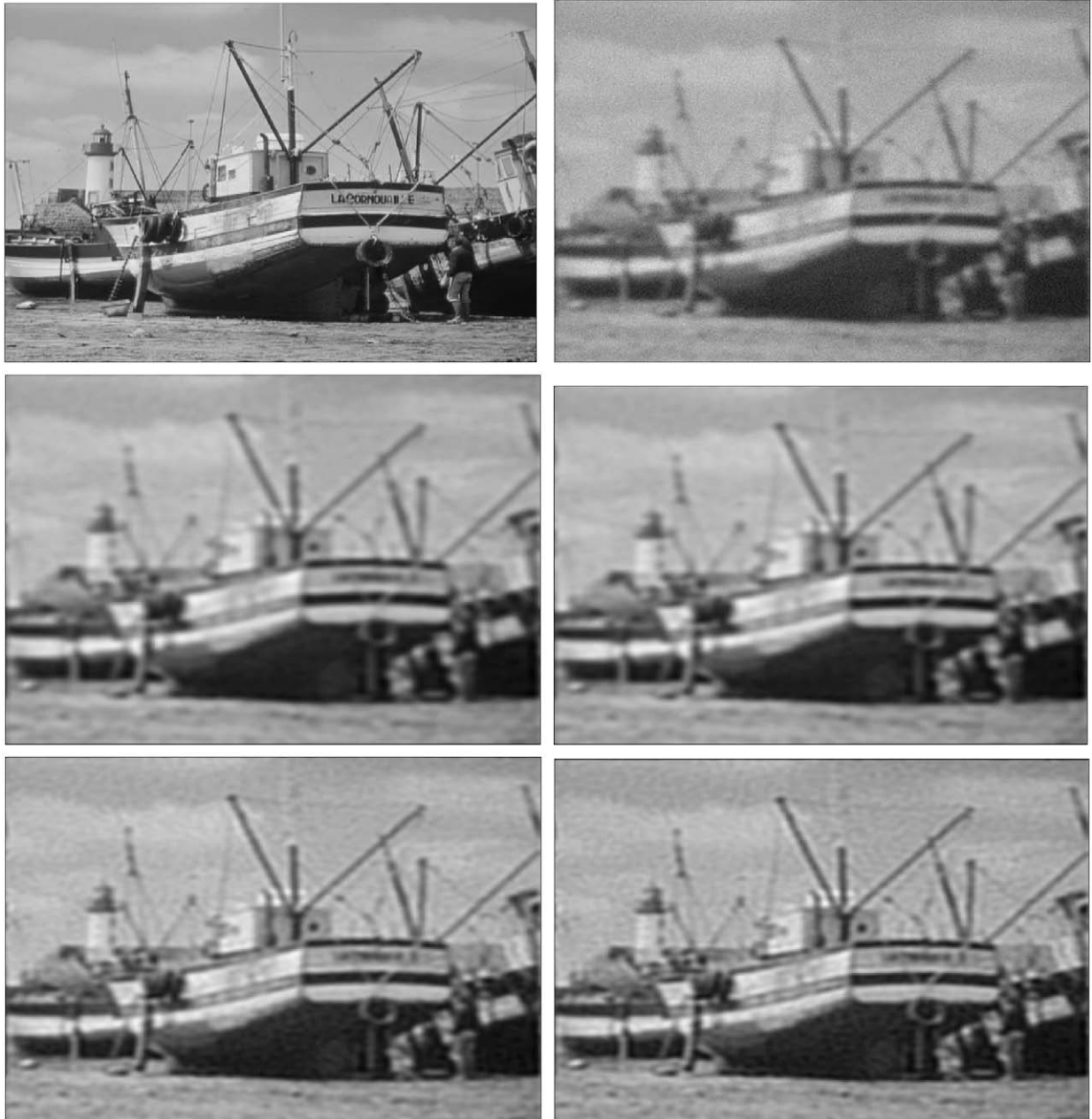


Fig. 6. “Boats” image—stronger degradation. Top left: original image. Top left: blurred noised image. Center left: restored by the Wiener deconvolution. Center left: restored by the regularized deconvolution. Bottom left: restored by the spline (order 2) deconvolution. Bottom right: restored by the spline (order 12) deconvolution.

regularity of the solution and the approximation of the initial data. The practical schemes for parameter choice are proposed in the paper. The solutions are derived in an explicit spline form using spline harmonic analysis presented in Section 3. This analysis provides a flexible computational scheme for the solution of the above problems. The order of the involved splines and the regularizing parameter can be adjusted when prior information on the properties of the sought after solution and the nature of the available data are unknown. We presented examples that demonstrate the application of the presented methods to restore some 1D signals and images from blurred and noised data.

The designed algorithms are easily implemented in a fast way while providing stable approximate solutions that restore the exact solutions with a great accuracy even when the initial data is severely corrupted by noise. The algorithm is able to resolve angles and peaks in signals, which are blurred in the initial data. It should be noted that the algorithm provides approximate solutions, which have the same smoothness as the exact solution. When the data is acquired from the measurement and there is no explicit a-priory knowledge, it is advisable to use the low-order splines when the noise and blurring are not strong and the original data can comprise sharp edges or (and) fine texture. On the other hand, when the noise and (or) blurring are strong then the higher order splines produce better results. The flexibility of the algorithm and its adaptation capabilities result in better performance compared to the related methods such as the Wiener deconvolution or the regularized deconvolution algorithm, which is used in the Matlab Image Processing toolbox, which is a particular case of our algorithm for the splines of order 1. We display in Figs. 5 and 6 the comparative deconvolution of the blurred and noised image “Boats” by the Wiener method, the Matlab regularized algorithm and our spline-based algorithm using the splines of order 2 and 12. The image in Fig. 5 was subjected to relatively weak blurring and noise degradation, while both these factors were much stronger for Fig. 6 image. In both cases the spline algorithms clearly outperformed the others. In the low-degraded case the order 2 spline produced the best result. When the degradation was strong, the order 12 spline algorithm outperformed all others. The PSNR values are given in Table 1. The numerical experiments definitely confirm these claims.

It should be noted that further improvement of the results can be achieved by application of some regularized version of the matching pursuit algorithm [9]. That

Table 1
PSNR values after deconvolution of the noised blurred “Boats” images by different methods.

Degraded	Wiener	Matlab-reg.	Spline 2	Spline 12
24.96	25.81	25.82	27.32	26.76
22.48	23.83	23.85	24.73	24.85

Top row—weakly degraded image, bottom row—strongly degraded image.

version (which is computationally more expensive compared to the presented technique) will be reported in our next publication.

Appendix A. Calculation of splines

In previous sections, we derived approximate solutions to the convolution equation and to the inversion of the heat equation in the form of periodic spline of order p

$$S^p(x) = \frac{1}{N} \sum_n \xi_n \beta_n^p(x) = \sum_{k \in \mathbb{Z}} q_k B^p\left(x - \frac{k}{N}\right), \quad \xi_n \triangleq \hat{q}(n),$$

$$q_k = \frac{1}{N} \sum_n \omega^{kn} \xi_n.$$

The value of the spline at any fixed point t_0 can be calculated using explicit form (up to periodization) of the B-spline

$$B^p(x) = \frac{N^p}{(p-1)!} \sum_{l=0}^p (-1)^l \binom{p}{l} \left(x - \frac{l}{N} + \frac{p}{2N}\right)_+^{p-1},$$

$$t_+ \triangleq \frac{t + |t|}{2}.$$

Recall that $N = 2^j$. The values of the spline at the sets of dyadic rational points $\{k/2^{j+l}\}$ can be calculated by subdivision using the coefficients $\{\xi_n\}$. For simplicity, we consider only splines of even order $p = 2r$.

The values of the spline at grid points are

$$S^p(k/N) = \frac{1}{N} \sum_n \xi_n \beta_n^p(k/N) = \sum_n \omega^{kn} \xi_n u_n^p. \tag{A.1}$$

We calculate the values of the spline on finer grids via the two-scale relation for the exponential splines β_n^{2r} . To highlight the scale we stay on, we introduce an additional index. In the rest of this section, $\beta_n^{2r,s}$, $u_n^{2r,s}$ and ξ_n^s mean β_n^{2r} , u_n^{2r} and ξ_n on the grid $\{k/2^s\}$.

Eq. (3.4) implies that

$$\begin{aligned} \beta_n^{2r,j}(x) &= \sum_{m=-\infty}^{\infty} e^{2\pi i(n+mN)x} \left(\frac{\sin(\pi(n+mN)/N)}{\pi(n+mN)/N}\right)^{2r} \\ &= \sum_{m=-\infty}^{\infty} e^{2\pi i(n+2mN)x} \left(\frac{2 \sin(2\pi(n+2mN)/2N)}{\pi(n+2mN)/2N}\right)^{2r} \\ &\quad + \sum_{m=-\infty}^{\infty} e^{2\pi i(n+N+2mN)x} \left(\frac{2 \sin(2\pi(n+N+2mN)/2N)}{\pi(n+N+2mN)/2N}\right)^{2r} \\ &= \cos^{2r} \frac{\pi n}{2N} \sum_{m=-\infty}^{\infty} e^{2\pi i(n+m2N)x} \left(\frac{\sin(2\pi(n+2mN)/2N)}{\pi(n+2mN)/2N}\right)^{2r} \\ &\quad + \cos^{2r} \frac{\pi(n+N)}{2N} \sum_{m=-\infty}^{\infty} e^{2\pi i(n+N+m2N)x} \\ &\quad \times \left(\frac{\sin(2\pi(n+N+2mN)/2N)}{\pi(n+N+2mN)/2N}\right)^{2r} \\ &= \cos^{2r} \frac{\pi n}{2N} \beta_n^{2r,j+1}(x) + \cos^{2r} \frac{\pi(n+N)}{2N} \beta_{n+N}^{2r,j+1}(x). \end{aligned} \tag{A.2}$$

The two-scale relation (A.2) enables to represent the spline S^{2r} on a finer grid

$$S^{2r}(x) = \frac{1}{2N} \sum_{n=0}^{N-1} \xi_n^j \left(\cos^{2r} \frac{\pi n}{2N} \beta_n^{2r,j+1}(x)\right)$$

$$\begin{aligned}
 & + \cos^{2r} \frac{\pi(n+N)}{2N} \beta_{n+N}^{2r,j+1}(x) \\
 = & \frac{1}{2N} \sum_{n=0}^{2N-1} \zeta_n^{2r} \cos^{2r} \frac{\pi n}{2N} \beta_n^{2r,j+1}(x).
 \end{aligned}$$

We recall that the sequence ζ_n^j is $N = 2^j$ -periodic.

By continuing the refinement, we obtain a representation of the spline S^{2r} on the grid $k/2^{j+s}$

$$S^{2r}(x) = \frac{1}{2^s N} \sum_{n=0}^{2^{j+s}-1} \zeta_n^{2r,s} \beta_n^{2r,j+s}(x),$$

$$C_n^{2r,s} \triangleq \prod_{l=1}^s \cos^{2r} \frac{\pi n}{2^{l+s}}.$$

Consequently, in order to produce values of the spline S^{2r} on the grid $k/2^{j+s}$, it is sufficient, like in (A.1), to implement the inverse FFT

$$S^{2r}(k/2^{j+s}) = \sum_{n=0}^{2^{j+s}-1} e^{2\pi i kn/2^{j+s}} \zeta_n^{2r} C_n^{2r,s} u_n^{2r,j+s}.$$

Appendix B. Convergence of approximate solutions to the exact solution of the convolution equation

In this section, we provide a proof to Theorem 4.1, which was formulated in Section 4.2.

Notation We denote by W_2^m the Hilbert space consisting of 1-periodic functions, whose derivatives up to order $m - 1$ are absolutely continuous while the m -th derivative is square summable on the interval $[0, 1]$. The norm in this space is

$$\|f\|_m \triangleq \sqrt{\sum_{i=0}^m \int_0^1 (f^{(i)}(x))^2 dx}.$$

In particular, $W_2^0 = L_2$. Obviously, $C^m \subset W_2^m$.

Let $\mathbf{y} = \{y_k\}_{k=0}^{N-1}$ be a data sequence. From now on we denote by $S^p(\mathbf{y}, x)$ the spline from \mathcal{S}^p , which interpolates \mathbf{y} on the grid $\{k/N\}_{k=0}^{N-1}$: $S^p(\mathbf{y}, k/N) = y_k$.

B.1. Auxiliary results

In this section, several facts are established that enable to prove the main result.

Lemma B.1. Assume $f \in W_2^m$ and $\mathbf{f} \triangleq \{f(k/N)\}_{k=0}^{N-1}$. Then, for $i = 0, \dots, m$, the following inequalities are true:

$$\|S^{2m}(\mathbf{f}, x)^{(i)}\| \leq \frac{1}{U_{2m}} \|f^{(i)}\|, \tag{B.1}$$

where U_{2m} is the constant defined in (3.6).

Proof. For $i = m$, Eq. (B.1) is equivalent to the well-known extremal property of the interpolatory splines (see [1], for example). To extend the inequality to $i < m$, we first note that, if $j > l$, then $u_n^{2j} < u_n^{2l}$, $n = 0, \dots, N - 1$. It follows from Eq. (3.5). Due to Eq. (3.16), $S^{2m}(\mathbf{f}, x) = \sum_n \beta_n^{2m}(x) \hat{f}(n) / u_n^{2m}$.

Then, Eqs. (3.15) and (3.6) imply that

$$\begin{aligned}
 \|S^{2m}(\mathbf{f}, x)^{(i)}\|^2 & = \sum_n w_n^{2i} |\hat{f}(n)|^2 \frac{u_n^{2(2m-i)}}{(u_n^{2m})^2} \\
 & < (U_{2m})^{-2} \sum_n w_n^{2i} |\hat{f}(n)|^2 \frac{u_n^{2i}}{(u_n^{2i})^2} \\
 & = (U_{2m})^{-2} \|S^{2i}(\mathbf{f}, x)^{(i)}\|^2 \leq (U_{2m})^{-2} \|f^{(i)}\|^2. \quad \square
 \end{aligned}$$

Proposition B.1 (Ahlberg et al. [1], p. 168). Assume $f \in W_2^m$. Then, there exist functions $d_i(f, x)$ and constants d_i , which do not depend on N , such that

$$S^{2m}(\mathbf{f}, x)^{(i)} = f^{(i)}(x) + N^{i-m+1/2} d_i(f, x),$$

$$|d_i(f, x)| \leq d_i \|f^{(m)}\|. \tag{B.2}$$

Lemma B.2. Assume $f \in W_2^m$. Then, there exist constants K_N and K such that

$$\|S^{2m}(\mathbf{f}, x)\|_m \leq K_N \|f(x)\|_m \leq K \|f(x)\|_m,$$

$$\lim_{N \rightarrow \infty} K_N = (U_{2m})^{-1}. \tag{B.3}$$

Proof. Eq. (B.2) implies that $\|S^{2m}(\mathbf{f}, x)\| \leq \|f(x)\| + d_0 \|f^{(m)}\|$. Using the inequality $2ab \leq ca^2 + c^{-1}b^2$, we get

$$\|S^{2m}(\mathbf{f}, x)\|^2 \leq (U_{2m})^{-2} \|f(x)\|^2 + \frac{N^{1-2m} (U_{2m})^2}{1 - (U_{2m})^2} d_0^2 \|f^{(m)}\|^2.$$

Thus, using Eq. (B.1), we obtain

$$\begin{aligned}
 \|S^{2m}(\mathbf{f}, x)\|_m^2 & \leq (U_{2m})^{-2} \|f(x)\|_m^2 \\
 & + \frac{N^{1-2m} (U_{2m})^2}{1 - (U_{2m})^2} d_0^2 \|f^{(m)}\|^2 \leq K_N^2 \|f(x)\|_m,
 \end{aligned}$$

$$K_N \triangleq \sqrt{(U_{2m})^{-2} + \frac{N^{1-2m} (U_{2m})^2}{1 - (U_{2m})^2} d_0^2}, \quad \lim_{N \rightarrow \infty} K_N = (U_{2m})^{-1}. \quad \square$$

The following fact is well-known (see, for example, [13]).

Proposition B.2. Assume $f \in W_2^r$. Then

$$S^r(\mathbf{f}, x) = f(x) + N^{-r} R(f, x),$$

$$|R(f, x)| \leq R \|f^{(r)}\|_\infty. \tag{B.4}$$

Here the constant R does not depend on f and N and $\|G\|_\infty \triangleq \max_{x \in [0,1]} |G(x)|$.

All previous facts are needed to establish the following main result in this section. Recall that $g(x) = h \star f(x)$. We introduce the spline of order $2m + r$

$$Q^{2m+r}(x) \triangleq S^{2m}(\mathbf{f}, x) \star S^r(\mathbf{h}, x),$$

$$\mathbf{Q}_N \triangleq \{Q^{2m+r}(k/N) - g(k/N)\}_{k=0}^{N-1}.$$

Lemma B.3. Assume $f \in W_2^m$. Then, there exists a constant $T(h)$, which depends on the kernel $h(x)$ but not on N , such that

$$\|\mathbf{Q}_N\| \leq N^{-s} T(h) \|f\|_m, \quad s \triangleq \min\{r, m - 1/2\}. \tag{B.5}$$

Proof. It follows from Eqs. (B.2) and (B.4) that

$$Q^{2m+r}(x) = g(x) + T(f, h, x),$$

$$\begin{aligned}
T(f, h, x) &\triangleq N^{-r} f \star R(h, x) + N^{-m+1/2} h \star d_0(f, x) \\
&\quad + N^{-m-r+1/2} R(h, x) \star d_0(f, x), \\
|T(f, h, x)| &\leq N^{-r} R \|f\| \|h^{(r)}\|_{\infty} + N^{-m+1/2} d_0 \|f^{(m)}\| \|h\|_{\infty} \\
&\quad + N^{-r-m+1/2} R d_0 \|h^{(r)}\|_{\infty} \|f^{(m)}\| \\
&\implies |Q^{2m+r}(x) - g(x)| \leq N^{-s} T(h) \|f\|_{\infty}, \quad (\text{B.6})
\end{aligned}$$

where the constant $T(h)$ does not depend on N . Hence, inequality (B.5) follows. \square

We recall that the available data are $\mathbf{z} = \mathbf{g} + \mathbf{e}$, where $\mathbf{e} = \{e_k\}_{k=0}^{N-1}$ is the sequence of errors.

Corollary B.1. Let $E(S^{\rho})$ be the functional defined in Eq. (4.1). Assume that the inequality $\|\mathbf{e}\| \leq \varepsilon$ holds. Then

$$E(S^{2m}(\mathbf{f}, \cdot)) \leq (\varepsilon + N^{-s} T(h) \|f\|_{\infty})^2. \quad (\text{B.7})$$

Proof. We have

$$\begin{aligned}
E(S^{2m}(\mathbf{f}, \cdot)) &= \frac{1}{N} \sum_k \left(S^r(\mathbf{h}, \cdot) \star S^{2m}(\mathbf{f}, \cdot) \left(\frac{k}{N} \right) - g \left(\frac{k}{N} \right) - e_k \right)^2 \\
&\leq (\varepsilon + N^{-s} T(h) \|f\|_{\infty})^2. \quad \square
\end{aligned}$$

Recall that the function $e(\rho) \triangleq E(S_{\rho}^{\rho})$ grows strictly monotonically, while $e(0) = \mu(z)$ and $\lim_{\rho \rightarrow \infty} e(\rho) = \|\mathbf{z}\|^2$ ($\mu(z) \triangleq \sum_{n \in \theta} |z(n)|^2$), where θ is the set of indices where $\hat{h}(n) = 0$. On the other hand, the function $i(\rho) \triangleq I(S_{\rho}^{2m}) = \|(S_{\rho}^{2m})\|_{\infty}^2$ (see Eq. (4.7)) decays strictly monotonically, while $i(0) = K$. Hence, it follows that the following equation:

$$e(\rho) = \left(\varepsilon + N^{-s} \frac{T(h)}{\sqrt{K}} \sqrt{i(\rho)} \right)^2 + \mu(z), \quad (\text{B.8})$$

has a unique solution for any ε such that

$$\varepsilon^2 + \mu(z) < \|\mathbf{z}\|^2.$$

Here K is the constant defined in Eq. (B.3).

B.2. Proof of the main result (Theorem 4.1)

In this section, we assume that the step $1/N$ of the grid and the norm of the error array $\|\mathbf{e}\|$ tend to zero. We describe how to select the parameter ρ in order for the solution S_{ρ}^{2m} of Problem MFC to converge to the function f .

Recall that C^n is the space of 1-periodic functions having continuous derivatives up to order n . The norm in this space is

$$\|F\|_{C^n} = \max_{i=0:n} \max_{x \in [0,1]} |F^{(i)}(x)|.$$

Let $N_j \triangleq 2^j$ and $\{\varepsilon_j\}$ be a sequence such that $\lim_{j \rightarrow \infty} \varepsilon_j = 0$. Let ρ_j be a root of Eq. (B.8) when $N = N_j$ and $\varepsilon = \varepsilon_j$. Let $\mathbf{e}_j \triangleq \{e_k\}_{k=0}^{N_j-1}$ be an array of errors such that $\|\mathbf{e}_j\| \leq \varepsilon_j$. Let $\mathbf{h}_j \triangleq \{h(k/N_j)\}_{k=0}^{N_j-1}$ and $\mathbf{z}_j \triangleq \{z_k^j\}_{k=0}^{N_j-1} = \{g(k/N_j)\}_{k=0}^{N_j-1} + \mathbf{e}_j$. Denote by $S_j(x)$ the spline of order $2m$ with nodes on the grid

$\{k/N_j\}$, which minimizes the functional

$$\begin{aligned}
J_j(S) &\triangleq \rho_j I_j(S) + E_j(S), \quad I_j(S) \triangleq \|S\|_{\infty}^2, \\
E_j(S) &\triangleq \frac{1}{N_j} \sum_{k=0}^{N_j-1} (S \star S(\mathbf{h}, \cdot)(k/N_j) - z_k^j)^2.
\end{aligned}$$

Remark. Assume that all the Fourier coefficients of the kernel $h(x)$ are non-zero. Then, Eq. (2.2) has a unique solution $f(x)$. In addition, this fact implies that, when j is sufficiently large, all the DFT coefficients $\hat{h}_j(n)$ of the array \mathbf{h}_j are non-zero. Then, for these j , $\mu(z) = 0$.

Lemma B.4. Assume that all the Fourier coefficients of the kernel $h(x)$ are non-zero and $\mu(z) = 0$. Then, all the splines $S_j(x)$ satisfy the inequality

$$\|S\|_{\infty} \leq \sqrt{K} \|f\|_{\infty},$$

where K is the constant defined in Eq. (B.3).

Proof. Since the spline $S_j(x)$ minimizes the functional $J_j(S)$ on the space \mathcal{S}^{ρ_j} , we get, by using Eqs. (B.3) and (B.7)

$$\begin{aligned}
J_j S_j &\leq J_j(S^{2m}(\mathbf{f}, \cdot)) = \rho_j \|S^{2m}(\mathbf{f}, \cdot)\|_{\infty}^2 + E(S^{2m}(\mathbf{f}, \cdot)) \\
&\leq \rho_j K \|f\|_{\infty}^2 + \left(\varepsilon_j + N_j^{-s} \frac{T(h)}{\sqrt{K}} \sqrt{K} \|f\|_{\infty} \right)^2.
\end{aligned}$$

From Eq. (B.8)

$$J_j(S_j) = \rho_j K \|S_j\|_{\infty}^2 + \left(\varepsilon_j + N_j^{-s} \frac{T(h)}{\sqrt{K}} \|S_j\|_{\infty} \right)^2.$$

Hence, the inequality (2.6) follows. \square

Theorem B.1. Assume that all the Fourier coefficients of the kernel $h(x)$ are non-zero, and $\mu(z) = 0$. Let $f(x)$ be the unique solution of Eq. (2.2). Then, the sequence of splines $\{S_j\}$ of order $2m$ converges in the norm of C^{m-1} to the function $f(x)$.

Proof. Lemma B.4 claims that the splines sequence $\{S_j\}$ is bounded in the norm of W_2^m . Therefore, it is compact in the norm of C^{m-1} (see, for example, [5]). Consequently, there exists a subsequence $\{S_{j_n}\}$, which converges in this norm to a function $\tilde{f}(x) \in C^{m-1}$. We will show that $\tilde{f}(x) \equiv f(x)$. Since $f(x)$ is a unique solution for Eq. (2.2), then, it is sufficient to prove that $h \star \tilde{f}(x) \equiv h \star f(x) = g(x)$. Denote

$$\begin{aligned}
D_1 &\triangleq \|h \star \tilde{f} - h \star S_{j_n}\|, \quad D_2 \triangleq \|S^r(\mathbf{h}, \cdot) \star S_{j_n} - h \star S_{j_n}\|, \\
D_3 &\triangleq \|S^r(\mathbf{h}, \cdot) \star S_{j_n} - S^{2m+r}(\mathbf{g}, \cdot)\|, \quad D_4 \triangleq \|g - S^{2m+r}(\mathbf{g}, \cdot)\|.
\end{aligned}$$

Obviously, the L_2 norm of the difference $\|h \star \tilde{f} - g\| \leq \sum_{i=1}^4 D_i$. We evaluate the differences D_i separately. The evaluation of the terms D_1 and D_2 is straightforward

$$\begin{aligned}
D_1^2 &\leq \|h\| \|\tilde{f} - S_{j_n}\| \rightarrow 0, \\
D_2^2 &\leq \|S^r(\mathbf{h}, \cdot) - h\| \|S_{j_n}\| \rightarrow 0 \quad \text{as } n \rightarrow \infty.
\end{aligned}$$

Inequality (3.18) implies that

$$D_3^2 \leq (U_{2m+r})^{-2} \frac{1}{N_{j_n}} \sum_{k=0}^{N_{j_n}-1} (S^r(\mathbf{h}, \cdot) \star S_{j_n}(k/N_{j_n}) - g(k/N_{j_n}))^2$$

$$\begin{aligned}
 &= (U_{2m+r})^{-2} \frac{1}{N_{j_n}} \sum_{k=0}^{N_{j_n}-1} (S^r(\mathbf{h}, \cdot) \star S_{j_n}(k/N_{j_n}) - z_k^{j_n} + e_k^{j_n})^2 \\
 &\leq \frac{2}{U_{2m+r}^2} (e(\rho_{j_n}) + \|\mathbf{e}_{j_n}\|^2) \\
 &\leq \frac{2}{U_{2m+r}^2} \left(\varepsilon_{j_n} + N_{j_n}^{-s} \frac{T(h)}{\sqrt{K}} \sqrt{i(\rho)^2 + \varepsilon_{j_n}^2} \right) \rightarrow 0 \text{ as } n \rightarrow \infty.
 \end{aligned}$$

The relation $\lim_{n \rightarrow \infty} D_4 = 0$ is obvious. Thus, we have $h \star \tilde{f}(x) \equiv h \star f(x) = g(x)$. Due to uniqueness of the solution of Eq. (2.2), we get $\tilde{f}(x) \equiv f(x)$. This remains true for any subsequence of the sequence $\{S^j\}$. Therefore, the whole sequence $\{S^j\}$ converges to f in the norm of C^{m-1} . \square

Remark on the uniqueness of the solution. Assume that some Fourier coefficients, whose indices constitute the set ϑ , are zero. Then, a solution of Eq. (2.2) exists if and only if the Fourier coefficients $\{\tilde{g}(n)\}_{n \in \vartheta} = 0$ of the data function g . If this is the case, then, the solutions to Eq. (2.2) are $f(x) = \tilde{f}(x) + \sum_{n \in \vartheta} b_n e^{2\pi i n x}$, where b_n are arbitrary numbers and $\tilde{f}(x)$ is the solution, which has a minimal norm. Then, the sequence $\{S^j\}$ converges to \tilde{f} in the norm of C^{m-1} .

References

[1] J.H. Ahlberg, E.N. Nilson, J.L. Walsh, *The Theory of Splines and their Applications*, Academic Press, New York, 1967.
 [2] A. Averbuch, V. Zheludev, Construction of biorthogonal discrete wavelet transforms using interpolatory splines, *Appl. Comput. Harm. Anal.* 12 (2002) 25–56.
 [3] C. Charles, G. Leclerc, P. Louette, J.-P. Ranson, J.-J. Pireaux, Noise filtering and deconvolution of XPS data by wavelets and Fourier transform, *Surf. Interface Anal.* 36 (2004) 71–80.
 [4] D.L. Donoho, Nonlinear solution of linear inverse problems by wavelet-vaguelette, *Appl. Comput. Harm. Anal.* 2 (1995) 101–126.
 [5] N. Dunford, J.T. Schwartz, *Linear Operators*, Interscience, New York, 1963.

[6] J. Fan, J.-Y. Koo, Wavelet deconvolution, *IEEE Trans. Inf. Theory* 48 (3) (2002) 734–747.
 [7] A.J.E.M. Janssen, The Zak transform: a signal transform for sampled time-continuous signals, *Philips J. Res.* 43 (1988) 23–69.
 [8] R. Lattès, J.-L. Lions, *Méthode de Quasi-Réversibilité et Applications*, Dunod, Paris, 1967.
 [9] S. Mallat, Z. Zhang, Matching pursuit with time-frequency dictionaries, *IEEE Trans. Signal Process.* 41 (12) (1993) 3397–3415.
 [10] R. Neelamani, H. Choi, R. Baraniuk, ForWaRD: Fourier-wavelet regularized deconvolution for ill-conditioned systems, *IEEE Trans. Signal Process.* 52 (2) (2004) 418–433.
 [11] D.L. Philips, A technique for the numerical solution of certain integral equations of the first kind, *J. Assoc. Comput. Mach.* 9 (1) (1962) 84–97.
 [12] I.J. Schoenberg, *Cardinal Spline Interpolation*, CBMS, SIAM, Philadelphia, vol. 12, 1973.
 [13] V.M. Tikhomirov, Best methods of approximation and interpolation of differentiable functions in the space $C[-1, 1]$, *Mat. Sb. (N.S.)* 80 (122) (1969) 290–304 (Russian).
 [14] A.N. Tikhonov, Solution of incorrectly formulated problems and the regularization method, *Sov. Math. Dokl.* 4 (1963) 1035.
 [15] A.N. Tikhonov, V.Y. Arsenin, *Solution of Ill-Posed Problems*, Wiley, New York, 1977.
 [16] N. Wiener, *Extrapolation, Interpolation and Smoothing of Stationary Time Series with Engineering Applications*, Wiley, New York, 1949.
 [17] J. Zak, Finite translations in solid-state physics, *Phys. Rev. Lett.* 19 (4) (1967) 1385–1387.
 [18] V.A. Zheludev, An operational calculus connected with periodic splines, *Sov. Math. Dokl.* 42 (1991) 162–167.
 [19] V.A. Zheludev, Periodic splines and the fast Fourier transform, *Comput. Math. Math. Phys.* 32 (1991) 149–165.
 [20] V.A. Zheludev, Spline-operational calculus and inverse problem for heat equation, in: J. Szabados, K. Tandoi (Eds.), *Proceedings of the International Conference on Approximation Theory, Kecskemét, Hungary, 1990*, *Colloq. Math. Soc. J. Bolyai* 58 (1991) 763–783.
 [21] V.A. Zheludev, Periodic splines, harmonic analysis, and wavelets, in: Y.Y. Zeevi, R. Coifman (Eds.), *Signal and Image Representation in Combined Spaces*, 477–509, *Wavelet Anal. Appl.*, 7, Academic Press, San Diego, CA, 1998.
 [22] V.A. Zheludev, Integral representation of slowly growing equidistant splines, *Approximation Theory Appl.* 14 (4) (1998) 66–88.
 [23] V.A. Zheludev, Wavelet analysis in spaces of slowly growing splines via integral representation, *R. Anal. Exch.* 24 (1998/99) 229–261.